Imaging analysis of digital holography

Lei Xu,[*] Xiaoyuan Peng, Zhixiong Guo,[*] Jianmin Miao, Anand Asundi

[*] *School of Engineering, Rutgers, the State University of New Jersey, Piscataway, NJ 08854*
School of Mechanical and Aerospace Engineering, Nanyang Technological University, Singapore, 639798
I.Leixu@osa.org

Abstract: In this study we focus on understanding the system imaging mechanisms given rise to the unique characteristic of discretization in digital holography. Imaging analysis with respect to the system geometries is investigated and the corresponding requirements for reliable holographic imaging are specified. In addition, the imaging capacity of a digital holographic system is analyzed in terms of space-bandwidth product. The impacts due to the discrete features of the CCD sensor that are characterized by the amount of sensitive pixels and the pixel dimension are quantified. The analysis demonstrates the favorable properties of an in-line system arrangement in both the effective field of view and imaging resolution.

© 2005 Optical Society of America

OCIS codes: (090.0090) Holography; (070.2580) Fourier optics; (110.2960) Image analysis; (120.3940) Metrology

References and links

1. U. Schnars and W. P. O. Juptner, "Digital recording and numerical reconstruction of holograms," Measurement Science and Technology **13,** R85-R101 (2002).
2. J. L. Valin, E. Goncalves, F. Palacios and J. R. Perez, "Methodology for analysis of displacement using digital holography," Optics and Lasers in Engineering **43**, 99-111 (2005).
3. I. Takahashi, T. Nomura, Y. Morimoto, S. Yoneyama and M. Fujigaki, "Deformation measurement by digital holographic interferometry," in *Optomechatronic Systems IV***,** George K. Knopf, eds., Proc. SPIE **5264**, 206-213 (2003).
4. J. R. Perez, E. Goncalves, R. De Souza, F. Palacios, M. Muramatsu, J. L. Valin and R. Gesualdi, " Two-source method in digital holographic contouring," in *5th Iberoamerican Meeting on Optics and 8th Latin American Meeting on Optics, Lasers, and Their Applications*, Aristides Marcano O. and Jose Luis Paz, eds., Proc. SPIE **5622**, 1422-1427 (2004).
5. P. Ferraro, G. Coppola, D. Alfieri, S. De Nicola, A. Finizio and G. Pierattini, "Recent advancements in digital holographic microscopy and its applications," in *Optical Metrology in Production Engineering*, Wolfgang Osten and Mitsuo Takeda, eds., Proc. SPIE **5457**, 481-491 (2004).
6. O. Matoba and B. Javidi, "Optical security in data communication and display," in *Optical Information Systems*, Bahram Javidi and Demetri Psaltis, eds., Proc. SPIE **5202**, 68-75 (2003).
7. E. Cuche, F. Bevilacqua and Ch. Depeursinge, "Digital holography for quantitative phase-contrst imaging," Opt. Lett. **24**, 291-293 (1999).
8. J. W. Goodman, *Introduction to Fourier Optics* (The McGraw-Hill Companies, Inc. New York, 1996).
9. Z. L. Yu and G. F. Jin, *Optical information processing* (Tsinghua University Press, Beijing, 1987).
10. L. Xu, J. Miao and A. Asundi, "Properties of digital holography based on in-line configuration," Opt. Eng. **39**, 3214-3219 (2000).
11. L. Xu, X. Peng, J. Miao and A. Asundi, "Studies of digital microscopic holography with applications to microstructure testing," Appl. Opt. **40**, 5046-5051 (2001).
12. L. Xu, X. Peng, A. Asundi, and J. Miao, "Digital microholointerferometer: development and validation," Opt. Eng. **42**, 2218-2224 (2003).

#6591 - $15.00 US Received 11 February 2005; revised 17 March 2005; accepted 18 March 2005
(C) 2005 OSA

1. Introduction

Digital holography [1] has been attracting intensive research efforts during recent years due to its potentials in automated high-resolution deformation measurement [2-3] and shape analysis [4], microscopic imaging and testing [5], as well as information transfer, storage and display [6], etc. The favorable imaging properties of holography are well utilized in these applications. Furthermore supported by digital recording and numerical evaluation, the imaging performance is advanced in terms of stability tolerance, direct data processing, phase-contrast imaging [7] and availability of high-quality phase variations. Serving as the basis of these features, analysis of digital holographic imaging is of great importance. In this paper, we study the distinct effects of discretization in digital holography on system imaging. The imaging mechanism and imaging capacity regarding different recording geometries are particularly analyzed. In addition, the impacts induced by a CCD sensor that is characterized by the sensitive pixel amount and pixel dimension to the image formation and quality are quantified.

In digital holography, the continuous spatial distribution of an optically generated hologram is sampled by the discrete sensitive pixels on a CCD array, whose outputs are converted to the digitized signals and stored in an image processing system for numerical evaluation. Such digital sampling principle and the subsequent matrix-based numerical processing result in new effects related to discretization non-existent in conventional holographic methods. Due to the particular effects, specific impacts are introduced to the system imaging mechanism and performance, regarding different system geometries. For precise recovery of an object by digital holography, the Whittaker-Shannon sampling theorem [8] implies that a band-limited function can be reconstructed from an appropriately spaced array of its sampled values. From a practical point of view, the distribution function of a hologram has significant spectrum values only in some finite regions, and hence can be treated to be approximately band-limited. Let's consider a space-limited function $g(x, y)$, which is approximately band-limited with an area range of $W_x \times W_y$ in the spectrum domain. According to the sampling theorem, the total amount of the sampling points, namely the space-bandwidth product, is given by $SW = L_x L_y W_x W_y$, where $L_x L_y$ is the spatial dimension of $g(x, y)$.

Space-bandwidth product is a physical quantity that is tightly related to information capacity. 120It can be applied to characterize the capability of the systems in information transferring and processing; and thus, it is a measure to evaluate the imaging quality. Specifically for digital holography, the imaging performance can be studied in term of the space-bandwidth product, which is determined by its effective field of view and the cut-off frequency. To record an object with holography, it is required that the SW of the system should be greater than that of the object so as to ensure no loss of information. Therefore, the space-bandwidth product of the input functions that will be accepted by the system can be employed to demonstrate its imaging performance. In this paper, the variations of SW of an object during the process of holographic recording are analyzed, based on which the discretization effects on digital holographic imaging are studied.

2. Diffraction and interference analysis

Suppose in the one-dimensional case, a test object has a lateral dimension of L_O and a spatial frequency bandwidth of W_O. Its space-bandwidth product, denoted as SW_O, is then given as $SW_O = L_O W_O$. In a Fresnel digital holography system, the object beam diffracts at an angle [9] $\alpha(\gamma_O) = \lambda \gamma_O$, where λ is the working wavelength and γ_O the spatial frequency of the object. In the hologram plane located at a distance D away from the object, the lateral

#6591 - $15.00 US Received 11 February 2005; revised 17 March 2005; accepted 18 March 2005
(C) 2005 OSA

displacement of the diffraction beam is equal to $\lambda D\gamma_O$. That means that the beam interacting with the object at point x_O with a spatial frequency γ_O will be incident in the hologram plane at the position $x_H = x_O + \lambda D\gamma_O$ as shown in Fig. 1. The propagation of the object beam can be briefly described in terms of the lateral location and the spatial frequency as

$$(x_O, \gamma_O)_O \rightarrow (x_O + \lambda D\gamma_O, \gamma_O)_H. \tag{1}$$

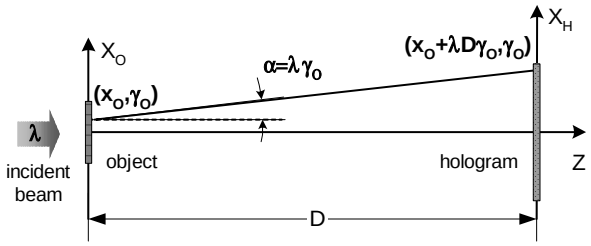

Fig. 1. Propagation sketch of the object beam

In the hologram plane where a CCD sensor is arranged, the superposition of the object wave O_H and an in-line reference wave R_H produces an intensity distribution that can be expressed by

$$h(x_H) = |O_H|^2 + |R_H|^2 + 2O_H R_H \cos(2\pi\gamma_O x_H). \tag{2}$$

Therefore the space-bandwidth product of an in-line hologram is given by

$$SW_{H:in-line} = SW_O \cdot (1 + \frac{\lambda D W_O}{L_O}). \tag{3}$$

Equation (3) represents the requirement on the information capacity of an in-line digital holography system. It should have a space-bandwidth product at least equal to that of the hologram. Otherwise, an object cannot be recovered reliably.

Consider the case of an off-axis arrangement. By offsetting the object at an angle θ along one coordinate axis, say the X-axis, the interference of the object wave with a normally incident reference wave results in a hologram given as

$$h(x_H) = |O_H|^2 + |R_H|^2 + 2O_H R_H \cos[2\pi(\gamma_O + \gamma_\theta)x_H], \tag{4}$$

where, $\gamma_\theta = \sin\theta / \lambda$ is the spatial frequency introduced by the offset angle. It implies that the variation of the SW of an object in the hologram plane occurs in both the lateral dimension and spatial frequency. The procedure can be described as

$$\begin{cases} x_O \rightarrow x_H = x_O + \lambda D\gamma_O, \\ \gamma_O \rightarrow \gamma_H = [-(\gamma_O + \gamma_\theta), 0, (\gamma_O + \gamma_\theta)]. \end{cases} \tag{5}$$

Figure 2 shows the shape sketches of the space-bandwidth product for both of the hologram types. Compared with the more compact feature of an in-line digital hologram, it is seen in the off-axis case that the two image terms shift apart to the central frequencies of $\pm\gamma_\theta$, respectively. Moreover, their SW shapes are no longer rectangular as that of the original object. Accordingly, CCD sensors that normally have a rectangular SW shape cannot be efficiently utilized.

Mathematically, an off-axis digital hologram has a space-bandwidth product given as

$$SW_{H:off-axis} = (L_O + \lambda D W_O) \cdot (W_O + 2\gamma_\theta). \tag{6}$$

#6591 - $15.00 US Received 11 February 2005; revised 17 March 2005; accepted 18 March 2005
(C) 2005 OSA

To ensure the spatial frequency components within W_O not affected by the quadratic noises, γ_θ has to satisfy $\gamma_\theta \geq \frac{3}{2}W_O$. Therefore, the minimum value of Equation (6) is

$$SW_{H:off-axis} = 4SW_O \cdot (1 + \frac{\lambda D W_O}{L_O}). \tag{7}$$

For a same object, this equation implies that an off-axis holography system must provide a space-bandwidth product that is at least a factor of four greater than that needed in an in-line arrangement so as to include the entire components of SW_H .

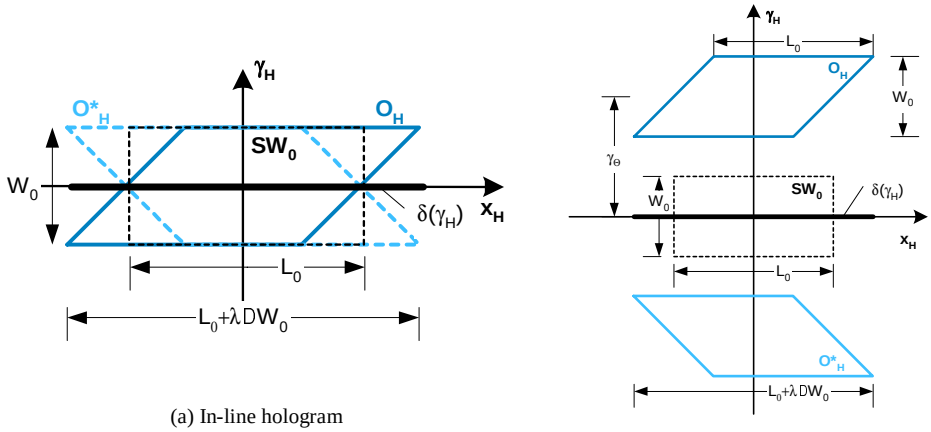

(a) In-line hologram

(b) Off-axis hologram

Fig. 2. Space-bandwidth product of a digital hologram

Comparison of Equation (3) and (7) gives the difference on the requirements for imaging the object information in the two types of system geometries. Originally, the information capacity of an object is an inherent property determined by the spatial dimension and bandwidth of itself. However, when the object is imaged by a digital holography system, constraints are applied to both the object size and the allowable spatial frequency due to the discretization effects. The effective field of view of the system confines the lateral dimension of an object that can be imaged. And the spatial bandwidth that can be transferred reliably is dependent on the system parameters. Therefore, studies on the imaging capacity of a digital holography system are needed by taking into account the different system configurations.

3. Imaging capacity of digital holography systems

In digital holography, whether the information of a test object can be reliably recorded and reconstructed depends on the capability of a system in resolving the micro interference patterns formed by the reference wave and all the point sources over the lateral extension of the object. However, for a CCD sensor that has a limited spatial resolution, the arrangement of the system has to be adjusted accordingly, so as to adapt the resultant fringe spacing to the spatial resolution of the CCD array used.

According to the recording mechanism of Fresnel digital holography [10], it is known that for a test object, there is a minimum recording distance allowed to arrange the object in order to fit the effective field of view of the system. For an in-line system, the effective field of view $L_x \times L_y$, as show in Fig. 3, is determined by the discrete features of the CCD sensor that are characterized by the pixel amount $N_x \times N_y$ and pixel size $\Delta N_x \times \Delta N_y$ as

#6591 - $15.00 US
Received 11 February 2005; revised 17 March 2005; accepted 18 March 2005
(C) 2005 OSA

$$L_x \times L_y = (\frac{\lambda D}{\Delta N_x} - N_x \cdot \Delta N_x) \times (\frac{\lambda D}{\Delta N_y} - N_y \cdot \Delta N_y). \tag{8}$$

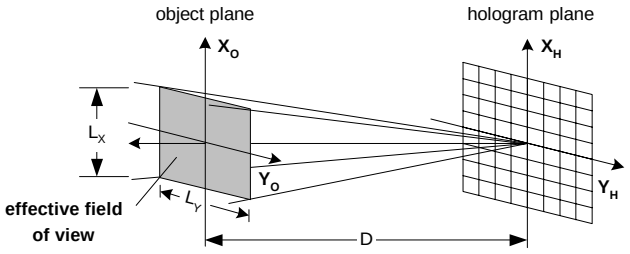

Fig. 3. Effective field of view of an in-line Fresnel digital holography system

For an off-axis arrangement, since digital imaging of an object has to meet simultaneously both the need of the minimum offset angle and the limitation of the maximum interference angle, the requirement of the recording distance is stricter in comparison with that of an in-line system. The effective field of view is just one-fourth of $(L_x \times L_y)_{in-line}$.

The distance corresponding to an effective field of view determines the highest achievable lateral resolution of an object with the maximum lateral extension L_O inscribed to the rectangular area. It is the spatial bandwidth allowed by the system, which is given below for the two different holographic geometries as

$$\begin{cases} W_{O:in-line} = \dfrac{N}{L_O + N \cdot \Delta N}, \\ W_{O:off-axis} = \dfrac{N}{4L_O + N \cdot \Delta N}. \end{cases} \tag{9}$$

To evaluate the imaging performance of a digital holography system with the information capacity of an object that can be accepted, the space-bandwidth product in the two system arrangements are

$$\begin{cases} SW_{in-line} = \dfrac{N \cdot L_O}{L_O + N \cdot \Delta N}, \\ SW_{off-axis} = \dfrac{N \cdot L_O}{4L_O + N \cdot \Delta N}. \end{cases} \tag{10}$$

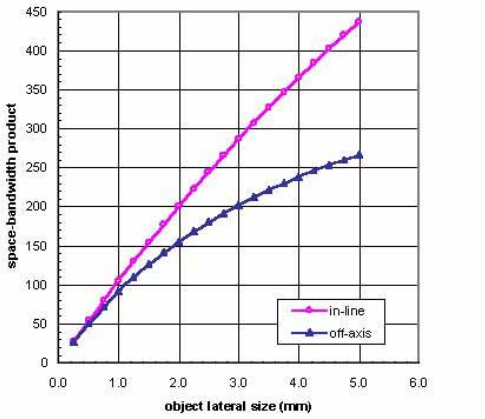

Fig. 4. Imaging capacity of digital holography systems

#6591 - $15.00 US
Received 11 February 2005; revised 17 March 2005; accepted 18 March 2005
(C) 2005 OSA

Equation (10) quantifies the effects given rise to the discretization on digital holographic imaging. The comparison of the two system arrangements is shown in Fig. 4 for the case of $N = 2048$ and $\Delta N = 9\mu m$. In an in-line system, less constraint is applied to the effective field of view, which allows a test object to be imaged with higher resolution, and hence more details can be detected. This property can be utilized for applications in micromeasurement [11-12], in which imaging quality is essential for evaluating the performance of a metrological system.

4. Discretization effects

The characteristic of discretization in digital holography is introduced by the use of a CCD sensor to sample a hologram with a $N_x \times N_y$ array with sensitive pixels having a finite dimension of $\Delta N_x \times \Delta N_y$.

The size of the sensitive area of a CCD sensor, which is mainly dependent on the amount of the effective pixels $N_x \times N_y$, plays an important role in Fresnel numerical reconstruction to acquire an image with high lateral resolution. Besides that, $N_x \times N_y$ involves in the determination of the effective field of view of a digital holography system as well. It can be regarded as a system factor evaluating the imaging quality, which can be described below in term of the 2D space-bandwidth product for the two types of recording geometries as

$$\begin{cases} SW_{in-line} = [N_x - \dfrac{(N_x \cdot \Delta N_x)^2}{\lambda D}][N_y - \dfrac{(N_y \cdot \Delta N_y)^2}{\lambda D}], \\ SW_{off-axis} = \dfrac{1}{4}[N_x - \dfrac{(N_x \cdot \Delta N_x)^2}{\lambda D}][N_y - \dfrac{(N_y \cdot \Delta N_y)^2}{\lambda D}]. \end{cases} \tag{11}$$

To show the effect of $N_x \times N_y$, Fig. 5 illustrates the dependence of *SW* on the amount of sampling points of a CCD sensor. The involved quantities include $\lambda = 532nm$ and $\Delta N_x \times \Delta N_y = 9\mu m \times 9\mu m$. The recording distance $D = 450mm$ is shown as an example in the figure, but the general tendency can be observed.

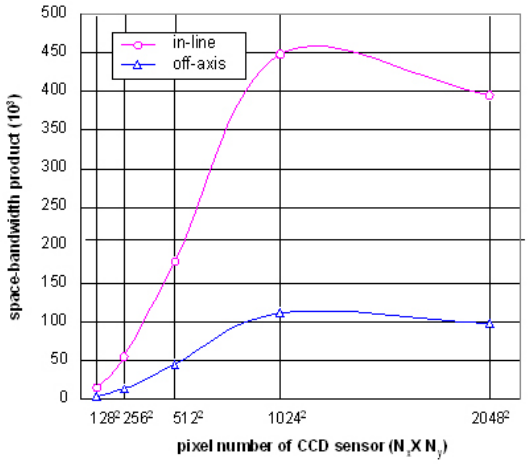

Fig. 5. Effect of sampling amount of CCD sensors

It is seen that the amount of sensitive pixels, to some extent, represents the imaging performance of a digital holographic system. More sampling points help to improve the

#6591 - $15.00 US Received 11 February 2005; revised 17 March 2005; accepted 18 March 2005
(C) 2005 OSA

system resolution and hence achieve higher imaging quality. However, it is noted in the figure that the space-bandwidth product has a maximum for the case of $N_x \times N_y = 1024 \times 1024$ pixels in this example. The reason for it is that a large chip aperture imposes tight constrains to the effective field of view. The integral imaging capacity of the system is degraded in spite of the increase in the lateral resolution. This study reveals the issue of efficient utilization of system capacity. In some applications where just a small recording distance *D* is allowed, it is possible that only a limited part of a CCD sensor can be used, while the remaining region that does not fulfill the sampling theorem makes no essential contribution to the reconstruction. In an in-line Fresnel system, the effective CCD aperture is given as $L_S^{'} = \lambda D / \Delta N - L_O$.

On the other hand, the simulation of digital sampling of the holograms with discrete points is an idealized situation. In reality, the sampling pulses always have finite area, corresponding to the pixel dimensions. Consider a sample pulse with the extension $\Delta N_x \times \Delta N_y$ representing a cell in a CCD chip. The intensity distribution $h(x_H, y_H)$ will then be integrated over the cell. Introducing the rectangular function, the integral over the CCD sensor can be written as

$$\begin{aligned} h(x_H, y_H) &= \iint_{\pm\infty} rect(\frac{x_H - \xi}{\Delta N_x}) rect(\frac{y_H - \eta}{\Delta N_y}) h(\xi, \eta) d\xi d\eta \\ &= rect(\frac{x_H}{\Delta N_x}) rect(\frac{y_H}{\Delta N_y}) \otimes h(x_H, y_H), \end{aligned} \tag{12}$$

where $\otimes$ is the convolution operator. This function is then sampled in the same way as in the ideal case. The reconstructed image wavefield now becomes

$$\begin{aligned} U(x_I, y_I) = (\Delta N_x \Delta N_y) Sinc(\Delta N_x \frac{x_I}{\lambda D}) Sinc(\Delta N_y \frac{y_I}{\lambda D}) \\ \cdot F\{h(x_H, y_H) \cdot \exp[\frac{j\pi}{\lambda D}(x_H^2 + y_H^2)]\} \\ \otimes (\Delta N_x \Delta N_y) comb(\Delta N_x \frac{x_I}{\lambda D}) comb((\Delta N_y \frac{y_I}{\lambda D}). \end{aligned} \tag{13}$$

where $F\{\}$ indicates the 2D Fourier transform.

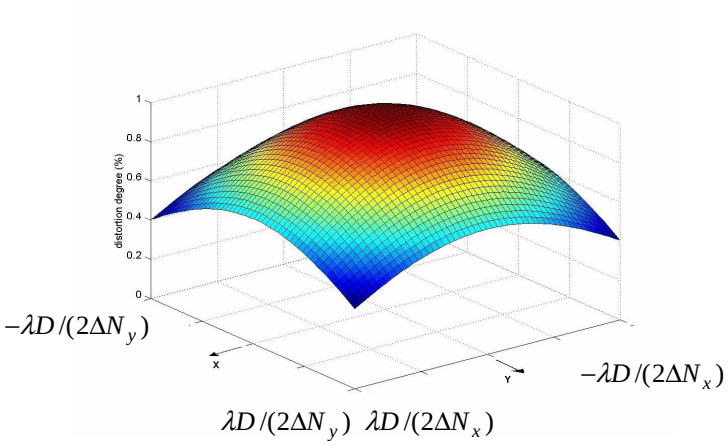

Fig.6. Intensity distortion in reconstructed images

#6591 - $15.00 US Received 11 February 2005; revised 17 March 2005; accepted 18 March 2005
(C) 2005 OSA

It is seen from the equation that the image is modified by a function over the reconstruction area. The influence of the function is on the amplitude term of the wavefield. Therefore, the non-ideal sampling effect induced by the finite pixel size of CCD sensors leads to the distortion of intensity distribution of an image. As shown in the Fig. 6, the intensity at the image corners is reduced to of the values for the ideal case. In practical applications when intensity is concerned, the distortion can be compensated by dividing the respective function from each pixel numerically. Nothing has to be done with it in the interferometric measurements since phase distribution is free from its influence.

The pixel dimension $\Delta N_x \times \Delta N_y$ determines the area of the reconstructed image, as well as the profile of the *Sinc* function. Studying the distortion gradient of the amplitude over the image area with respect to different pixel size, we obtain the relation curve shown in Fig. 7. It is obvious that CCD sensors having fine sampling pixels help to achieve reconstructed images with more uniform intensity distributions.

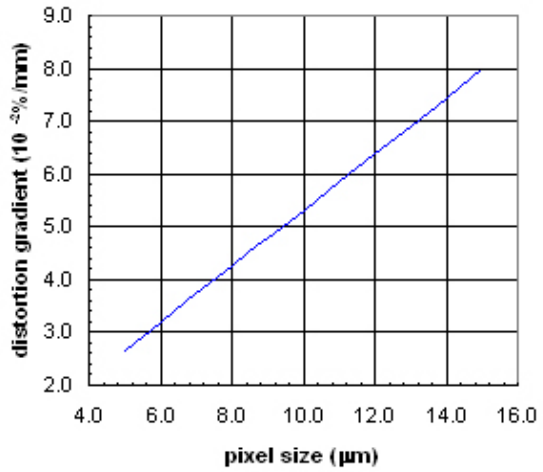

Fig. 7. Influence of pixel size on amplitude distortion

5. Conclusions

In conclusion, for the applications of digital holography, especially in the field of micromeasurement, studies on imaging performance are of particular importance. Given rise to the unique characteristic of discretization in digital holography, the system imaging mechanisms are studied in this paper. Through the analysis on the variation of the information capacity of an object during the process of diffraction and interference recording, the imaging requirements, regarding both the in-line and off-axis digital holography geometries, are demonstrated. Moreover, the imaging capacity of a digital holography system is quantitatively evaluated in terms of space-bandwidth product, taking into account the effects due to the discrete features of the CCD sensor that are characterized by the sensitive pixel amount and the pixel size. It is concluded from the analysis that, an in-line system can exhibit better performance, both in terms of a larger effective field of view and a higher imaging resolution.

In studies of the image formation and quality of a digital holography system, the effects introduced by the discretization characteristics of a CCD sensor are discussed. By quantifying the contribution of the amount of sampling pixels to the space-bandwidth product of a system, it is found that, the N, characterizing the CCD chip aperture, describes the information capacity of a system. However, it is worthwhile to mention that imaging performance is an integral quantity of both the effective field of view and imaging resolution. The application of

#6591 - $15.00 US Received 11 February 2005; revised 17 March 2005; accepted 18 March 2005
(C) 2005 OSA

a sensor array needs to coordinate the requirements in both aspects. On the other hand, it is found that the sensitive extension of a sampling pixel contributes to the amplitude distortion of a reconstructed image, in which the four corners are affected most with an intensity decrease to 40.53% .

#6591 - $15.00 US Received 11 February 2005; revised 17 March 2005; accepted 18 March 2005
(C) 2005 OSA